MULTI-BUMP, BLOW-UP, SELF-SIMILAR SOLUTIONS OF THE COMPLEX GINZBURG-LANDAU EQUATION

C. J. BUDD [*], V. ROTTSCHÄFER [†], AND J. F. WILLIAMS [‡]

Abstract. In this article we construct, both asymptotically and numerically, multi-bump, blow-up, self-similar solutions to the complex Ginzburg-Landau equation in the limit of small dispersion. Through a careful asymptotic analysis, involving a balance of both algebraic and exponential terms, we determine the parameter range over which these solutions may exist. Most intriguingly, we determine a branch of solutions that are not perturbations of solutions to the nonlinear Schrödinger equation, moreover, they are *not monotone* but they are *stable*. Furthermore, these ring-like solutions exist over a broader parameter regime than the monotone profile.

1. Introduction. The complex Ginzburg-Landau equation (CGL),

$$i\frac{\partial \Phi}{\partial t} + (1 - i\varepsilon)\nabla^2\Phi + (1 + i\delta)|\Phi|^2\Phi = 0, x \in \mathbf{R}^d, t > 0 \qquad (1.1)$$

arises as a model equation in a variety of problems from physics, biology and chemistry. These include nonlinear optics, models of turbulence, Rayleigh-Bénard convection, superconductivity, superfluidity, Taylor-Couette flow and reaction-diffusion systems, see [18, 2, 23, 7, 8] and in particular the review article [1]. The CGL can be seen as a normal form that describes the leading order behaviour of small perturbations in 'marginally unstable' systems of nonlinear partial differential equations defined on unbounded domains, [17]. Hence, it is relevant for understanding the dynamics of 'instabilities' in a wide variety of physical and other contexts. The coefficients in the equation can be expressed in terms of the coefficients of the underlying system of PDE's and thus their meaning depends on the problem at hand. As such, in this paper we would like to consider the dynamics of the CGL for a wide range of parameters.

In the limit of $\varepsilon = \delta = 0$ the CGL reduces to the well known Nonlinear Schrödinger equation (NLS), which lies at the heart of many physical problems related to wave modulation. This limit can be obtained from the standard form of the complex Ginzburg-Landau equation

$$A_t = rA + (1 + ib)\nabla^2 A + (1 + ic)|A|^2 A, \qquad b, c \in \mathbf{R}$$

by rescaling and considering the limit $|b|, |c| \to \infty$. The case of $\varepsilon > 0$ which we consider in this paper is a dissipative perturbation of the NLS.

The cubic NLS has the important property that when posed in dimension $d \geq 2$, there are sets of initial data that lead to solutions which become infinite (blow-up) at a finite time T. This phenomenon is called *self-focusing* in the context of nonlinear optics and collapse when applied to problems on turbulence. We will study the related question of blow-up in the CGL in this article. We focus on $\varepsilon \ll 1$ and $\delta \ll 1$ to study the case where the CGL can be seen as a small perturbation of the NLS.

[*]Department of Mathematical Sciences, University of Bath, Bath BA2 7AY, UK (cjb@maths.bath.ac.uk).

[†] Mathematical Institute, Leiden University, P.O. Box 9512, 2300 RA Leiden, the Netherlands (vivi@math.leidenuniv.nl).

[‡] Mathematical Institute, Leiden University, P.O. Box 9512, 2300 RA Leiden, the Netherlands and Centrum voor Wiskunde en Informatica, PB 94079, 1090 GB Amsterdam, the Netherlands (williams@cwi.nl).

Blow-up in the NLS has been extensively studied by many authors, and a recent monograph [24] gives a survey of the current literature. The dimension $d = 2$ is critical for the cubic NLS and marks the boundary between blow-up and integrable behaviour. When $d = 2$ the singularity formation is *approximately self-similar* where $\|\Phi\|_\infty$ is believed to be proportional to $\log|\log(T-t)|(T-t)^{-1/2}$ [24, 15]. When $d > 2$ the blow-up takes a self-similar form with $\|\Phi\|_\infty$ proportional to $(T-t)^{-1/2}$ as $t \to T$. A proof of the existence and local uniqueness of radially symmetric, monotone, self-similar blow-up solutions for d close to 2 is given in [14], with an extension of this result given in [21]. In [4] and [3] numerical calculations supported by formal asymptotic calculations give evidence for the existence of further multi-bump, self-similar, blow-up solutions for $d > 2$ where multi-bump is in the sense that $|\Phi|$ may have many local maxima. Moreover, the existence and local uniqueness of these multi-bump, blow-up, self-similar solutions is proved in [22].

The NLS is an example of a Hamiltonian partial differential equation of hyperbolic type with various conserved quantities. Whilst $\|\Phi\|$ becomes singular at a single point, the unitary nature of the NLS implies that Φ has a constant L_2-norm (power) and a conserved Hamiltonian

$$H = \int |\nabla\Phi|^2 - \frac{1}{2}|\Phi|^4 \, dV. \tag{1.2}$$

In this article we will explore the non-trivial relationship between blow-up solutions in the CGL and the NLS. In particular, we determine for which values of the dimension d and the parameters ε and δ self-similar blow-up is observed. This relationship was firstly considered by Fibich and Levy [10] who looked at the CGL problem in the limit of small ε and δ by using modulation theory. Their analysis concentrates on the blow-up of solutions in *two dimensions*. In [11] the asymptotic results are extended by applying a modulational approach to general perturbations of NLS-type equations for fixed $d = 2$. The main result of this analysis was the observation that when $\alpha \equiv \varepsilon + 2\delta > 0$ there are *no stable blow-up solutions* which are modulated NLS blow-up solutions. Indeed, it is established that the solutions are bounded, for all time, by a term exponentially large in α^{-1}. In contrast, finite time blow-up is observed if $\alpha < 0$. The latter results are not unexpected since if we consider spatially uniform solutions then blow-up in the ODE $i\phi_t = -(1+i\delta)\phi|\phi|^2$ only occurs for $\delta < 0$. Similarly for $\varepsilon < 0$, the CGL is a non-dissipative perturbation of NLS, and is close to the backwards heat equation. What is remarkable is that blow-up can be observed if ε or δ are positive but *only for $d > 2$*. It is the range of values for which this occurs that is of interest to us in this article.

The radially symmetric, blow-up solutions of the CGL in dimensions d higher than 2, are already studied in [19]. There it is assumed that the blow-up profile is *self-similar* and a similarity reduction is made; we review this dynamical rescaling in Section 2. The rescaling reduces the study of the radially symmetric blow-up solutions of the CGL to that of a related second order complex ordinary differential equation combined with certain far field conditions on the solutions at infinity. Whilst no rigorous proof of the existence of the solutions of this ODE is available (although some partial results are known) strong numerical evidence reported in [19] indicates that when $d > 2$, the self-similar blow-up solutions of the NLS described in [3] smoothly perturb as ε, δ *increase* from zero, to give a family of multi-bump, self-similar, blow-up solutions. We show that for $\delta = 0$, multi-bump solutions appear to exist in a parameter range $0 \le \varepsilon \le \varepsilon_k^*(d)$ where $\varepsilon_k^*(d) \to 0$ as $d \to 2$ and k is an integer index denoting the

2
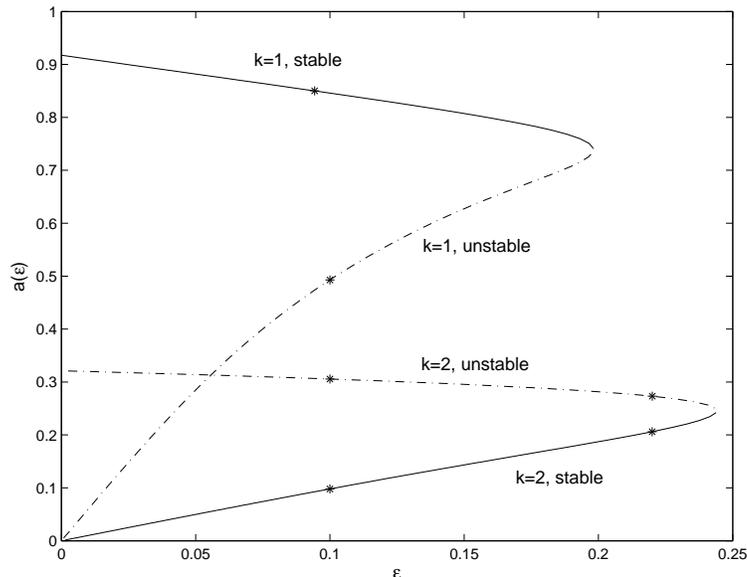
FIG. 1.1. *The $k = 1$ solution branch, the solutions with one maximum on $(-\infty, \infty)$, and the $k = 2$ solution branch, the solutions with two maxima on $(-\infty, \infty)$, plotted in the (ε, a)-plane where $d = 3$ and $\delta = 0$. The solutions corresponding to the *'s are given in Figure 1.2. On the upper part of the $k = 1$ solution branch and the lower part of the $k = 2$ solution branch the solutions are found to be stable whereas on the other parts the solutions are unstable.*

number of maxima of the modulus of a solution on the real line. Every k-solution branch consists of two parts which coalesce in a fold bifurcation at $\varepsilon = \varepsilon_k^*(d)$. The solutions on the upper part of the branch are smooth perturbations of the NLS self-similar solutions. In contrast, the solutions on the lower part of the branch, which tends weakly to zero as $\varepsilon \to 0$, are not a simple perturbation of the solutions of the NLS. In Figure 1.1, we give two of these branches where solutions are found in the (ε, a)-plane, these branches where obtained numerically, see Section 7. Here a is a small parameter that will appear when introducing the dynamical rescaling into the equation in Section 2. The two solution branches given in the figure correspond to solutions with one maximum at $\xi = 0$, $k = 1$, and with two maxima, $k = 2$, on the real line. The norm of the solutions that are found on the upper and lower part of both of the branches at $\varepsilon = 0.1$, the points indicated by the *'s, are given in Figure 1.2.

We present an asymptotic analysis which supports both the numerical results presented here and those in [19]. The form of the monotonically decreasing solution, $k = 1$, and the solution with two maxima on the real line, $k = 2$, is determined. Also, an indication of how to extend these results to a general k-solution is given. Furthermore, an asymptotic description of the branches of the various multi-bump solutions is obtained, including an estimate of the location of the fold bifurcation point $\varepsilon_k^*(d)$. An interesting feature of this calculation is that whereas the description of the solutions on the upper part of a branch (which are perturbations of the solutions of the NLS) is valid only for $d - 2$ small, the description of the solutions on the lower part of the branch remains valid in the case of quite general d (for small ε), including the physically interesting case of $d = 3$. A particular conclusion of the present study is
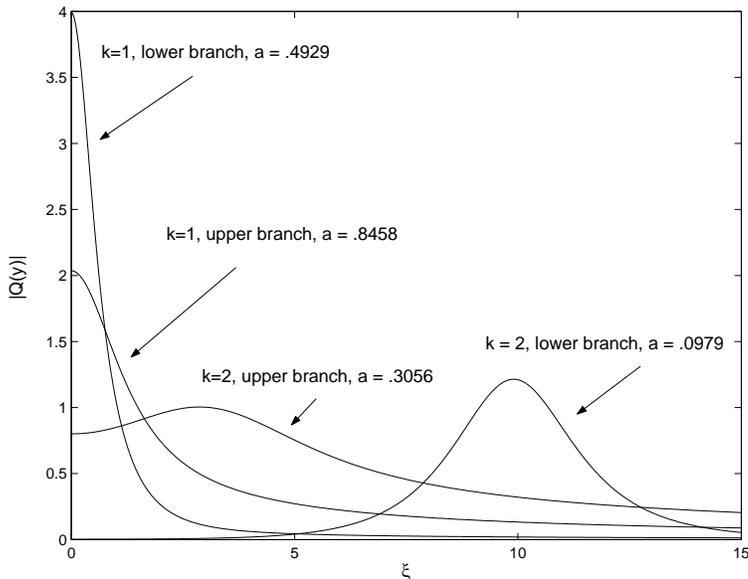
FIG. 1.2. *Final-time profiles in the rescaled variables for $d = 3, \delta = 0$ and $\varepsilon = 0.1$. The solutions correspond to the *'s in Figure 1.1*

the estimate for the location of the fold bifurcation. Whilst this can be in principle calculated for general δ it is easiest to express when $\delta = 0$.

PROPOSITION 1.1. *In the limit $d \to 2^+$, for the case of $\delta = 0$, the range of ε for which a multi-bump, self-similar, blow-up solution may exist on the k-solution branch, is given by $0 \le \varepsilon < \varepsilon_k^*(d)$, where*

$$\varepsilon_k^*(d) = C_k \frac{d - 2}{|\log(\frac{D_k}{d-2})|}, \tag{1.3}$$

to leading order Here $C_k > 0$ and $D_k > 0$ are constants that can be determined explicitly and that depend upon the structure of the solution. For instance, in the special case of a multi-bump solution with two maxima on the real line, for which $k = 2$, we have

$$\varepsilon_2^*(d) = \frac{\lambda_2(d - 2)}{\log(3\lambda_2/(d-2))} + \mathcal{O}\left(\frac{1}{\log(d-2)^2}\right), \tag{1.4}$$

where $\lambda_2 = \frac{2\pi}{3} - \frac{\sqrt{3}}{2}$.

In Table 1 in Section 3 a comparison is made between the asymptotic formula above and the results of numerical computations of the fold location for $k = 1$ and $k = 2$. These show excellent agreement.

We use a numerical method for ordinary differential equations (on infinite domains) to obtain the branches in Figure 1.1 and the solutions in Figure 1.2. Note that in Figure 1.1 the range of ε for which $k = 2$ solutions exist is larger than that of the monotone ($k = 1$) solutions. This leads to the question of stability of the solutions. In [19], stability is studied by numerically examining the spectrum of the linearization of

4

the computed solutions. We investigate this further by doing a numerical calculation of the radially symmetric forms of blow-up of the full partial differential equation (1.1). This simulation was suggested but not implemented in [19]. We use a *scale-invariant* adaptive numerical method that exploits scaling structures of the underlying equations to give an optimal temporal and spatial resolution of the solution as a blow-up singularity is approached. In particular we calculate solutions that grow in amplitude from their initial data by over nine orders of magnitude. This simulation allows us to determine both the stability of the various types of blow-up profiles and the effect of taking different initial data for varying values of ε, the results will be discussed in detail in Section 7. We find that the solutions on the upper part of the $k = 1$ solution branch and on the lower part of the $k = 2$ solution branch are stable. On the other part solutions are unstable. This is denoted in Figure 1.1 by the solid and dashed curves. Our most interesting observation is that the $k = 2$ solution is not only stable over a range of values of ε, but that it can be the only stable profile observed for certain ranges of ε, namely for $\varepsilon_1^*(d) < \varepsilon < \varepsilon_2^*(d)$. This is in complete contrast to blow-up in other systems such as NLS, the semilinear heat equation and chemotaxis amongst others where stable exact non-monotone, self-similar blow-up, profiles are not seen.

The layout of the remainder of this paper is as follows. In Section 2 we describe the basic scaling laws and self-similar profiles associated with blow-up in the CGL system. We state in Section 3 the main asymptotic result related to the behaviour of the solution branches. In Section 4 we analyze the phase of the solution which makes a matching possible between the far field solution and the solution close to the peaks. The monotone solution $(k = 1)$ is the subject of Section 5 and in Section 6 we focus on the self-similar, multi-bump solutions. In Section 7 we first determine the numerical solution of the ordinary differential equation that the self-similar solutions must satisfy. This allows us to determine the accuracy of the asymptotic calculation. We then apply a scale invariant adaptive method to find the time-dependent solutions of the full partial differential equation.

2. Blow-up and scaling laws. In this Section we consider the equations satisfied by the self-similar blow-up solutions of (1.1). We will assume that blow-up occurs at time T at the spatial origin and is radially symmetric. (In the case of the NLS such solutions are believed from numerical calculations reported in [24, 15] to be attractors.) Such solutions satisfy the partial differential equation

$$i\frac{\partial \Phi}{\partial t} + (1 - i\varepsilon)\left(\frac{\partial^2 \Phi}{\partial r^2} + (d-1)\frac{\partial \Phi}{\partial r}\right) + (1 + i\delta)|\Phi|^2\Phi = 0. \qquad (2.1)$$

In physical applications d will be an integer, however, it is very convenient for asymptotic analysis to consider the case of non-integer d. In particular, numerical calculations of solutions in the physically interesting case of $d = 3$ can be continuations of solutions determined when d is close to 2. Furthermore, keeping a cubic nonlinearity and varying d is essentially equivalent to fixing d and varying the nonlinearity.

In Figure 2.1, we give results of a numerical simulation of the CGL when starting with a monotone initial condition for $d = 3$ and $\varepsilon = 0.1$. In the physical coordinates the blowup occurs at the origin and in the rescaled variables (to be discussed below), we see convergence to a stationary profile.

It is easy to see that (2.1) is invariant under a change in the phase of the solution, also under a change in the scale of r, t and Φ or under a translation in time. That is,

5
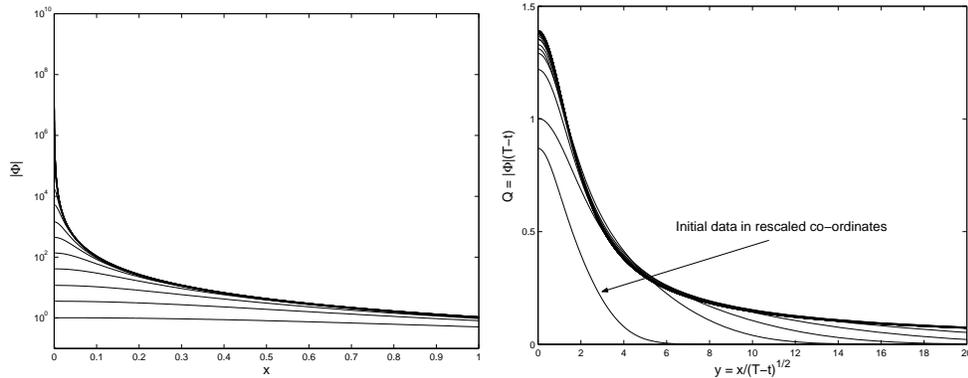
FIG. 2.1. *Numerical simulation of the full CGL for $d = 3$ and $\varepsilon = 0.1$. (left) Blow-up in physical coordinates. (right) Blow-up in rescaled coordinates, notice the convergence to a stationary profile.*

it is invariant under the continuous group of transformations

$$\Phi \mapsto e^{i\theta}\Phi, \quad \text{or} \quad t \mapsto \lambda t, \quad r \to \lambda^{1/2}r, \quad \Phi \to \lambda^{-1/2}\Phi \qquad \text{where } \lambda > 0.$$

Blow-up of the solution occurs at the origin for this equation at the blow-up time $T < \infty$ if

$$\max_r |\Phi(r,t)| = |\Phi(0,t)| \to \infty, \quad \text{as} \quad t \to T^-,$$

with $|\Phi(r,t)| < \infty$ for all $t < T$, $r \geq 0$ and $\lim_{t \to T^-} |\Phi(r,t)| < \infty$ for all $r > 0$.

In the NLS, blow-up occurs on a length scale $L(t)$ with $L(t) \to 0$ as $t \to T$ [24, 15]. We assume that similar behaviour occurs in the CGL. Accordingly, to resolve the temporal and spatial structure we introduce a dynamic rescaling of the solution so that space, time, and Φ are scaled by factors of $L(t)$, leading to a more regular equation. Taking

$$\xi \equiv \frac{|x|}{L(t)}, \ \tau \equiv \int_0^t \frac{1}{L^2(s)}ds, \ u(\xi,\tau) = L(t)\Phi(x,t), \tag{2.2}$$

the rescaled solution $u(\xi,\tau)$ satisfies the rescaled partial differential equation

$$iu_\tau + (1 - i\varepsilon)\left(u_{\xi\xi} + \frac{d-1}{\xi}u_\xi\right) + (1 + i\delta)|u|^2u + ia(\tau)(\xi u)_\xi = 0, \tag{2.3}$$

where

$$a = -L\frac{dL}{dt} = -\frac{1}{L}\frac{dL}{d\tau}.$$

The simplest form of blow-up behaviour, with $L(t) \to 0$ arises when $a(\tau)$ is a *positive* constant and

$$u(\xi,\tau) = e^{i\omega\tau}Q(\xi). \tag{2.4}$$

For simplicity we will consider only the case $\omega \equiv 1$. Although left in as an unknown constant by the authors in [19] this does not affect the solutions under consideration

6

as ω can easily be scaled out by scaling Q, ξ and a with ω. The resulting solutions are then precisely the *self-similar, blow-up solutions* which themselves are invariant under the group transformations. We have

$$L(t) = \sqrt{2a(T-t)} \quad \text{and} \quad \tau = \frac{\log(T-t)}{2a}, \tag{2.5}$$

and

$$(1 - i\varepsilon)\left(Q_{\xi\xi} + \frac{(d-1)}{\xi}Q_\xi\right) - Q + ia(\xi Q)_\xi + (1 + i\delta)|Q|^2 Q = 0. \tag{2.6}$$

The constant $a > 0$ above is a non-linear eigenvalue for the reduced equation (2.6) and represents a coupling between the length-scale and the phase. The value of a needs to be determined as part of the solution process.

Note that choosing different initial values for the PDE (2.1) will in general correspond to different values of $Q(0)$ and ω, where also $\omega \neq 1$ can be found. However, these all reduce to the same ODE (2.6). We will consider a solution to (2.6) to be stable if, in the limit $t \to T$ a solution of (1.1) converges to a solution of (2.6) under the rescalings (2.2) and (2.4).

In the rescaled equation (2.3), the perturbations in the CGL of the nonlinear and Laplacian terms of the NLS are given by $\delta u|u|^2$ and $\varepsilon \nabla^2 u$. As u and ξ are of unit order when blow-up is approached, these perturbations are of equivalent order provided that $\delta \sim \varepsilon$. This is the motivation to set

$$\delta = \Delta \varepsilon, \quad \Delta \in \mathbf{R}$$

and henceforth, without loss of generality, assume $\varepsilon \neq 0$. This balance between ε and δ is also found in formulae derived in [10] for the saturation of blow-up in CGL.

3. Admissible solution branches.

3.1. Existence of solution branches. The complex ordinary differential equation (2.6) must be satisfied by the self-similar solutions. Considered as an initial value problem, it has many solutions, and only those that satisfy certain conditions at infinity are admissible as being related to self-similar solutions of the partial differential equation. These conditions are the same as for the NLS to guarantee agreement in the limit $\varepsilon \to 0$. Briefly, the admissible solutions are those solutions of (2.6) that are *slowly varying* at infinity. More precisely, the initial and asymptotic conditions for a self-similar solution $\Phi(x, t)$ of the partial differential equation, namely that $\Phi(x, 0) = \Phi_0(x)$ and that $|\Phi|$ vanishes as $|x| \to \infty$, respectively, lead to the following initial and asymptotic conditions for $Q(\xi)$, respectively,

$$Q_\xi(0) = 0, \ \text{Im}\, Q(0) = 0, \tag{3.1}$$
$$|Q(\xi)| \to 0 \ \text{as} \ |\xi| \to \infty. \tag{3.2}$$

Here we have exploited the phase invariance of the differential equation to define the phase of Φ at the origin. Alternatively, we could have kept ω as an unknown in (2.4) and set $Q(0) = 1$ as in [19]. From a related regularity result, see [24], it also follows that

$$\left| \xi Q_\xi + \left(1 + \frac{i}{a}\right) Q \right| \to 0 \ \text{as} \ |\xi| \to \infty \tag{3.3}$$

7

must hold for solutions Φ with finite H^1 norm. In the NLS limit this corresponds to solutions with finite Hamiltonian H (1.2).

The majority of the solutions of (2.6) are rapidly varying as $|\xi| \to \infty$ and do not satisfy the condition (3.3). Such solutions are proportional to $\exp(ia\xi^2)$ in this limit and have unbounded H^1-norm. In contrast the slowly varying solutions (for both CGL and NLS) are polynomially decaying and

$$Q(\xi) \sim \frac{\mu}{\xi} \exp\left(-\frac{i}{a}\log(\xi)\right) = \mu\xi^{-1-\frac{i}{a}} \quad \text{as } \xi \to \infty. \tag{3.4}$$

The value of μ given by these solutions of (2.6) that are slowly varying at infinity, plays a central role in the later work on matching.

Monotone solutions

It is believed that the solutions of (2.6) that are slowly varying at infinity occur only for *isolated* values of the nonlinear eigenvalue a. However in the case that $|Q(\xi)|$ is a *monotonically decreasing* function of ξ (monotone solution) a proof of the existence and local uniqueness is only known for the NLS close to $d = 2$ and $a = 0$ [14, 21]. In particular, if $a = \varepsilon = \delta = 0$ then (2.6) reduces to

$$Q_{\xi\xi} + \frac{d-1}{\xi}Q_\xi - Q + |Q|^2Q = 0. \tag{3.5}$$

It is known that this equation has a discrete set of exponentially decaying solutions, of which the monotone decreasing solution is called the *ground state* or Townes soliton and is known to be unique [16]. For $a > 0$ and $\varepsilon = \delta = 0$ the following results are known about the monotone solutions of (2.6) satisfying the conditions (3.1) - (3.3) [24, 21],

THEOREM 3.1 (Sulem and Sulem, Rottschäfer and Kaper). *(i) As $d \to 2$ then there exists a monotone solution of the NLS with $a \to 0$, indeed,*

$$d - 2 \sim \frac{A}{a}e^{-\pi/a}, \tag{3.6}$$

(ii) For $d = 2 + \mathcal{O}(a^p)$ and a sufficiently small, a monotone solution of (2.6) exists and is locally unique.

Non-monotone solutions

In [3] the above result for the NLS is extended through a formal asymptotic argument that implies the existence of further *non-monotone* slowly varying solutions of (2.6). These have also been detected in numerical computations [4]. The computations reported in [19] indicate that similar solutions characterized by the number of turning points of the amplitude of $|Q|$, are found for CGL. Accordingly we define a k-solution branch to be a branch of solutions, denoted by $Q_k(\xi)$, for which $|Q_k|$ has k maxima on the whole real line $\xi \in (-\infty, \infty)$. (So that the monotone solutions lie on the $k = 1$ solution branch.) A particular conclusion of [3] was the existence of a $k = 2$ solution branch, where in the limit of $d \to 2$ there is a solution $Q_2(\xi)$ with a local minimum at $\xi = 0$ and isolated peaks at points asymptotically close to $|\xi| = 1/a$. In the limit of $d \to 2$ and $a \to 0$, this solution exists when

$$d - 2 \sim \frac{3}{a}e^{-\lambda_2/a} \quad \text{and} \quad \lambda_2 = 2\pi/3 - \sqrt{3}/2. \tag{3.7}$$
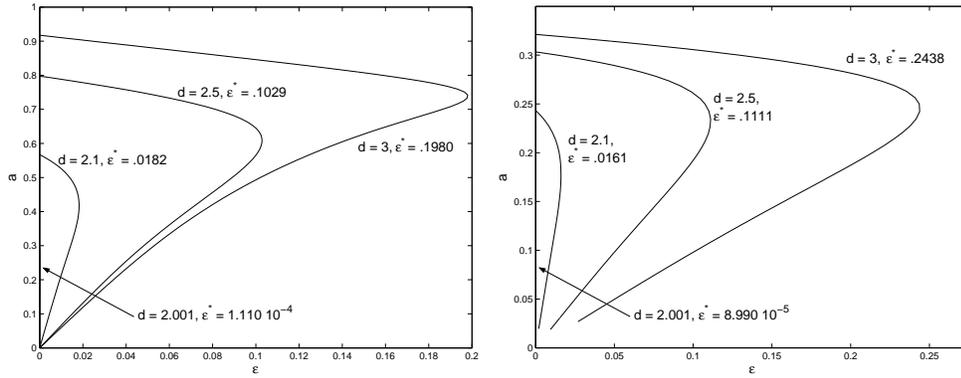
FIG. 3.1. *(left) The $k = 1$ solution branch, the monotone solution is found here, in the (ε, a)-plane for different choices of d where $\delta = 0$. (right) The $k = 2$ solution branch, the solution Q_2 with two maxima on the real line is found here, in the (ε, a)-plane for different choices of d where $\delta = 0$. The value of the fold bifurcation point $\varepsilon_k^*(d)$ is also given for the branches.*

There is no reason to expect that this is the only two-bump solution, in fact, the following existence and uniqueness result is also known [22]

THEOREM 3.2 (Rottschäfer and Kaper). *For each a sufficiently small, there exists a $n_0(a)$ such that, if $2 \leq n \leq n_0(a)$, then with $d = 2 + \mathcal{O}(a^l)$ for any $l > d + 1$ there exist $4(n-1)$ locally unique symmetric $2n - 1$-bump solutions with a maximum at $\xi = 0$ and $n - 1$ maxima for $\xi > 0$.*

While this theorem indicates that in the case of the NLS there are multiple multi-bump solutions, the construction in [22] shows that they are exponentially close to each other. While we anticipate that these families persist for ε and δ small but non-zero they cannot be distinguished by the asymptotics discussed in this paper and we denote any member of this family as "the k-bump solution". We show presently that we can extend both of the results (3.6) and (3.7) to the CGL system by looking at the limit of the solutions when the nonlinear eigenvalue a is *small*. In particular we have the following.

PROPOSITION 3.3. *For a and ε sufficiently small*

(i) There exists a branch of monotone solutions $(k = 1)$ which are smooth perturbations of the monotonically decreasing solution of the NLS. On this branch the values of a, d, ε and δ are related through the asymptotic formula

$$e^{-\lambda_1/a} = \left(C_1(d-2)a - C_2\varepsilon - C_3\delta\right)\left(1 + \mathcal{O}\left(a^2, a\varepsilon, a\delta\right)\right), \quad \lambda_1 = \pi/2 \qquad (3.8)$$

with explicitly computable constants $C_i(d) > 0$ for all d (defined in Section 5), and $C_3/C_2 \to 2$ as $d \to 2$.

(ii) There also exist k-solution branches, $k \geq 2$, on which the solutions $Q_k(\xi)$ with k maxima on the real line are found. Along every k-solution branch the values of a, d, ε and δ are related through

$$e^{-\frac{\lambda_k}{a}} = \left(C_{1,k}(d-2)a - C_{2,k}\varepsilon - C_{3,k}\delta\right)\left(1 + \mathcal{O}\left(a\right)\right), \qquad (3.9)$$

where the constants λ_k and $C_{i,k}$ can be computed from integrals of the solution $Q_k(\xi)$ along each branch.

9
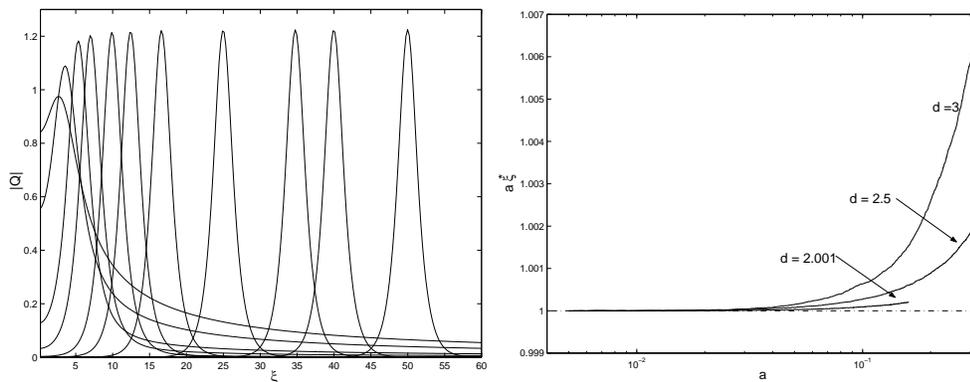
FIG. 3.2. *(left) The amplitude of the solutions* $|Q_2(\xi)|$ *for* $\xi > 0$ *as* a *and* ε *are moving along the* $k = 2$ *solution branch for* $d = 3$. *The peak of the solution moves to the right as* a *is decreased to zero. For smaller values of* a, *the solutions have a similar form and the peak* ξ^* *is located close to* $\frac{1}{a}$. *(right) The location of the maximum* ξ^* *along the* $k = 2$ *solution branch for various choices of* d *where* $a\xi^*$ *is plotted as a function of* a.

The solutions on the $k = 2$ *solution branch have a local minimum at the origin and maxima located at the points* $|\xi| = \mathcal{O}(\kappa/a)$ *where* κ *can be determined explicitly, and*

$$e^{-\lambda_2/a} = (C_{1,2}(d-2)a - C_{2,2}\varepsilon - C_{3,2}\delta)\left(1 + \mathcal{O}\left(a\right)\right) \tag{3.10}$$

For $\delta = 0$ *then*

$$\lambda_2 = 2\pi/3 - \sqrt{3}/2, \quad \kappa = 1, \quad and \quad C_{1,2} = C_{2,2} = 1/3.$$

In Section 6 we present the explicit computation of the coefficients in (3.9) where a $k = 2$ solution is constructed.

It is possible to consider the solutions as functions of d, ε and δ. In calculations it is convenient to fix d and δ and to vary the value of ε, the branches of the solutions can then be represented in a diagram by plotting the value of a. A numerical calculation of the $k = 1$ and $k = 2$ solution branches in the (ε, a)-plane is given in Figure 3.1 for a range of values of d, where $\delta = 0$. Also, the value of the fold bifurcation point $\varepsilon_k^*(d)$ is given for each of the branches. Note that the range of existence of the branch drops to zero as $d \to 2$.

In Figure 3.2 we plot the amplitude of the multi-bump solution $Q_2(\xi)$ on the $k = 2$ solution branch in the case of $d = 3, \delta = 0$ and we show how this solution changes along the branch. In this figure the peak of the solution moves uniformly to the right as a decreases along the branch (so that ε initially starts at zero, reaches a maximum at $\varepsilon_k^*(d)$ and then decreases to zero again as the peaks move to the right). The solution with the peak nearest to the origin is found for $\varepsilon = 0, a = 0.3124...$ which is the solution of the NLS computed in [4]. This solution does not have a form which is easy to analyse. In contrast, as a and ε tend to zero (along the solution branch), the solution takes on a localized form, with a peak located at a point ξ^* close to $1/a$. We demonstrate this in Figure 3.2 by plotting $a\xi^*$ as a function of a for various d. It is this solution with a peak located close to $\frac{1}{a}$, found on the lower part of the solution branch which is described by the asymptotic formula (3.10) and which will be analysed in detail in Section 6.

10
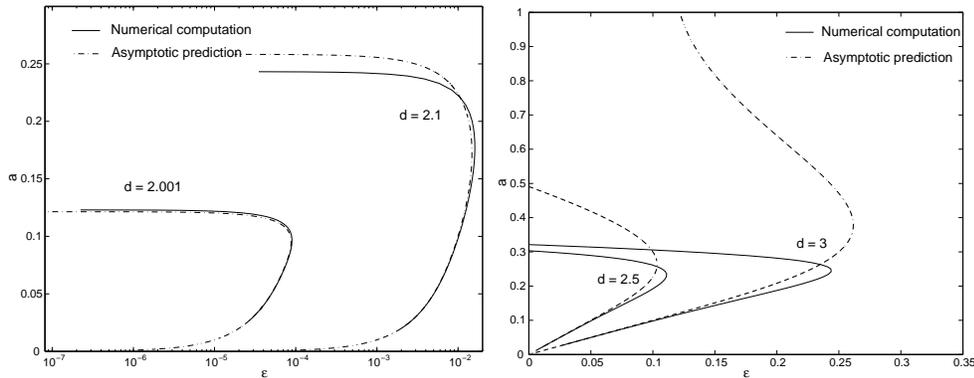
FIG. 3.3. *Comparison of the numerical results (solid line) and the asymptotic expansion for a_- and a_+ (dashed line) of the $k = 2$ solution branch. (left) Here $d = 2.1, 2.001$ and ε is plotted on a log-scale. (right) For $d = 2.5$ and $d = 3$.*

3.2. The existence of two solutions on each branch. In Figure 3.1 we clearly see that there exists a $\varepsilon_k^*(d)$, where the value of ε_k^* depends upon the branch, such that for every value of $\varepsilon < \varepsilon_k^*$ there are two solutions on each k-solution branch with corresponding values of a: $a_+ > a_-$. In fact, in the limit of $d \to 2$ and/or $\varepsilon \to 0$ we can determine, from the asymptotic formulae (3.8) and (3.10), both the two values a_- and a_+ and, the position of the fold asymptotically, for $\delta = 0$. More specifically, when we set $\varepsilon = 0$ and $\delta = 0$ in (3.9) we obtain an asymptotic expression for a_+ and when we set $a = 0$ and $\delta = 0$ in (3.9) we obtain an asymptotic expression for a_-:

$$a_+ \sim \frac{\lambda_k}{|\log(C_{1,k} a_+ (d-2))|} \quad \text{and} \quad a_- \sim \frac{\varepsilon A_k}{(d-2)}. \tag{3.11}$$

It is clear from comparing these results to with those of Theorem 3.1 that the solution corresponding to $a = a_+$ is a natural perturbation of the solution of the NLS in the limit of small ε. Moreover, a_+ is only small when $d - 2$ is small, and the asymptotic description of a_+ is only valid in this limit.

In contrast, the solution corresponding to $a = a_-$ is not a perturbation of the solution of the NLS. Furthermore, the value of a_- is small provided that ε is small, regardless of the value of $d - 2$; we may even take $d = 3$.

The agreement between the numerical results of the branches and the asymptotic calculations is very good indeed, as can be seen in Figure 3.3. There we present a plot comparing the values of a given in (3.11), to the numerically computed $k = 2$ solution branch for various values of d. We observe from this figure that the lower branch a_- is well approximated for a wide range of values of d provided that ε is small. In contrast, the upper branch a_+ is only well approximated when $d - 2$ is small.

This nice agreement for a_- leads us to believe that it may be possible to prove the existence of this part of the branch for general $2 < d < 4$ and, therefore, in the physically important case of three dimensions. We leave this as future work.

3.3. The position of the fold bifurcation. The two two parts of the branch corresponding to $a = a_+$ and $a = a_-$ coalesce in a fold bifurcation at the point (a_k^*, ε_k^*) and solutions for each of these parts of the branch only exist for $\varepsilon < \varepsilon_k^*$. We can derive

11

	$k = 1$		$k = 2$	
d	Asymptotic	Numerical	Asymptotic	Numerical
3	.1517	.1980	.2616	.2439
2.5	.0914	.1024	.1034	.1111
2.1	.0151	.0182	.0148	.0161
2.001	$9.177\ 10^{-5}$	$1.110\ 10^{-4}$	$8.770\ 10^{-5}$	$8.991\ 10^{-5}$

TABLE 3.1

Comparison of the asymptotic and numerical location of the fold point ε^* for $k = 1$ and $k = 2$ for various values of d with $\delta = 0$.

the estimates (1.3) and (1.4) for $\varepsilon_k^*(d)$ from the asymptotic results presented in (3.9) and (3.10). Indeed, differentiating (3.9) with respect to a and applying the condition

$$\frac{d\varepsilon}{da}(a_k^*) = 0,$$

determines (a_k^*, ε_k^*) exactly. In the case of $\delta = 0$, this condition yields that a_k^* satisfies the asymptotic relation

$$a_k^* = \frac{\lambda_k}{\log\left(\frac{\lambda_k}{C_{1,k}(d-2)}\right) - 2\log(a_k^*)}$$

so that as $d \to 2$ we have asymptotically

$$a_k^* \sim \frac{\lambda_k}{\log\left(\frac{\lambda_k}{C_{1,k}(d-2)}\right)}.$$

The critical value of ε for the k-solution branch is then determined by substituting the differentiated expression back into (3.9) as

$$\varepsilon_k^* = (d-2)\left(a_k^* - \frac{(a_k^*)^2}{\lambda_k}\right)\frac{C_{1,k}}{C_{2,k}}. \tag{3.12}$$

Combining these expressions gives (1.3) to leading order, where $\varepsilon_k^* \to 0$ as $d \to 2$.

In Table 3.1 we present a comparison of the asymptotic values of ε_k^* given by formula (3.12) with the numerical values for the $k = 1$ and $k = 2$ solution branches for various values of d. The agreement between the numerical and asymptotic calculations is excellent, especially when considering the various approximations that have been made to obtain the asymptotic formula for the fold location.

The restriction on the range of ε over which self-similar blow-up is observed is fully consistent with the calculations presented in [10] in the case of $d = 2$. In particular, we see that the range of the dissipative values of $\varepsilon > 0$ and $\delta > 0$ over which we see *self-similar* blow-up reduces to the empty set as $d \to 2$ when each branch collapses to a single point. In the case of $d = 2$ (when the blow-up of the NLS is marginal) we only see blow-up for the non-dissipative values of $\varepsilon, \delta < 0$ described in [10]. In contrast, for $d = 3$ (where blow-up is observed for the NLS) the range of ε values over which self-similar blow-up exists is quite large.

4. Construction of the asymptotic solution.

4.1. Overview. The construction of asymptotic solutions leading to the statements in Propositions 1.1 and 3.3 is similar to that described in [3], although rather more subtle as it involves both polynomial and exponential terms. In all parts of the analysis we presume that a is small, but in contrast to the NLS case described in [3] we do not necessarily require that $d - 2$ is also small. The calculation is rather different for the case of the monotone solutions on the $k = 1$ solution branch compared to that for the multi-bump solutions on the other branches, although both follow similar lines.

The solutions are constructed by determining them on three distinct ranges of ξ which are then matched to eachother. Firstly we examine the far field solution when $a\xi \gg 1$. Then, the solution is small and equation (2.6) can be approximated by a linear equation. Secondly, we determine global estimates on the evolution of the phase of the solution that allow a comparison between the form of the solution for the large values of $a\xi$ described above and smaller values of $a\xi$. Next we construct an inner solution valid over the range $a\xi \ll 1$. Similar to the cases described in [3], this solution is either a regular perturbation of the monotone decreasing ground state solution of (3.5) or it is an exponentially growing perturbation of the ground state or the zero solution. However, these exponentially growing perturbations are only small if $a\xi$ is small. The regular perturbations of the ground state solution lead to monotone solutions of the CGL, whereas the exponentially growing perturbations lead to multi-bump solutions of the CGL related to those described in [3]. In the case of the monotone solutions we match an exponentially decay in the solution for $a\xi < 2$ with a polynomial decay when $a\xi > 2$ by using a WKB analysis. In contrast, the exponentially growing perturbations lead to multi-bump solutions and we study these in the vicinity of the isolated peaks which occur when $a\xi = \mathcal{O}(1)$. Following this analysis we again match a solution decaying exponentially away from the peak for $a\xi < 2$ with a polynomial decay when $a\xi > 2$ by using a WKB analysis.

4.2. Far-field behaviour $a\xi \gg 1$. We now consider the behaviour of Q for large values of $a\xi$. The boundary condition (3.2) requires that $|Q|$ is very small in this range of ξ values and, therefore, equation (2.6) can be closely approximated by the linearized equation

$$(1 - i\varepsilon)\left(Q_{\xi\xi} + \frac{d-1}{\xi}Q_\xi\right) - Q + ia(\xi Q)_\xi = 0. \tag{4.1}$$

This equation is also obtained after rescaling in ξ with $\sqrt{1 - i\varepsilon}$ in the far field equation that is satisfied by the solutions of the NLS (when $\varepsilon = 0$). The solutions to that equation for the NLS are parabolic cylinder functions that now must be rescaled. For small ε, the solutions of (4.1) change type when $a\xi = 2$ (as in the NLS case), admitting exponentially decaying solutions for $a\xi < 2$ and polynomially decaying solutions for $a\xi > 2$. Applying the rescaling of ξ to the solutions given in [3] implies that there are (complex) constants μ, ν such that as $a\xi \to \infty$ (so that $a\xi > 2$) and ε small

$$Q(\xi) \sim \mu \xi^{-1-i/a}\left(1 + \mathcal{O}\left(\frac{1}{a\xi^2}\right)\right)$$

or

$$Q(\xi) \sim \nu \xi^{1-d+i/a} e^{-ia\xi^2/2} e^{a\varepsilon\xi^2/2}\left(1 + \mathcal{O}\left(\frac{1}{a\xi^2}\right)\right).$$

13

Of these two solutions, the first is slowly varying and decaying, whereas the second is rapidly varying and growing when $\varepsilon > 0$. Only this first solution can be matched to the boundary conditions satisfied by a self-similar solution and the consequent far field condition for $Q(\xi)$ given in (3.4). Consequently, if we decompose Q in amplitude and phase as

$$Q(\xi) = A(\xi)\exp\left(i\int_0^\xi \psi(x)dx\right) \tag{4.2}$$

then for $a\xi \gg 1$

$$A \approx \frac{\mu}{\xi}\left(1 + \mathcal{O}\left(\frac{1}{a\xi^2}\right)\right) \quad \text{and} \quad \psi \approx -\frac{1}{a\xi}\left(1 + \mathcal{O}\left(\frac{1}{a\xi^3}\right)\right). \tag{4.3}$$

4.3. Global estimates. We can link the far field solution to the global behaviour of Q via a rigorous result that relates the amplitude and phase of the solutions of (2.6). This relation is central in our final analysis and we will state it here. Substituting the decomposition (4.2) of Q in amplitude and phase into (2.6) leads to the following expression for A and ψ

$$A_{\xi\xi} = \psi^2 A - \frac{d-1}{\xi}A_\xi + A - A^3$$
$$- \varepsilon\left(2A_\xi\psi + A\psi_\xi + \frac{d-1}{\xi}A\psi\right) + a\xi A\psi \tag{4.4}$$

$$\psi_\xi = -2\psi\frac{A_\xi}{A} - \frac{d-1}{\xi}\psi + \frac{\varepsilon}{A}\left(A_{\xi\xi} - A\psi^2 + \frac{d-1}{\xi}A_\xi\right)$$
$$- \frac{a}{A}(A + \xi A_\xi) - \Delta\varepsilon A^2, \tag{4.5}$$

where $\delta = \Delta\varepsilon$. From this system we obtain the following integral equation for ψ

LEMMA 4.1. *The phase ψ and the amplitude A satisfy*

$$\psi + \frac{a\xi}{2} = \frac{1}{\xi A^2}\int_0^\xi \left((2-d)A^2\psi + \varepsilon x A\left(A_{xx} - A\psi^2 + \frac{d-1}{x}A_x\right) - \Delta\varepsilon x A^4\right) dx. \tag{4.6}$$

Proof. Consider first the identity

$$\frac{d}{dx}\left(xA^2\left(\psi + \frac{ax}{2}\right)\right) = (A^2 + 2xAA_x)\left(\psi + \frac{ax}{2}\right) + xA^2\left(\psi_x + \frac{a}{2}\right)$$
$$= (A^2 + 2xAA_x)\left(\psi + \frac{ax}{2}\right) + xA^2\left[\frac{a}{2} - 2\psi\frac{A_x}{A} - \frac{d-1}{x}\psi\right.$$
$$\left. + \frac{\varepsilon}{A}\left(A_{xx} - A\psi^2 + \frac{d-1}{x}A_x\right) - \frac{a}{A}\left(A + xA_x - \Delta\varepsilon A^2\right)\right]$$
$$= (2-d)\psi A^2 + \varepsilon x A\left(A_{xx} - A\psi^2\right) + \frac{d-1}{x}A_x - \Delta\varepsilon x A^4.$$

Integrating this identity from 0 to ξ and using the fact that $\psi(0) = 0$ we obtain the statement of the lemma. $\qquad\square$

14

From Lemma 4.1 and the asymptotic estimates (4.3), it follows that for $a\xi \gg 1$

$$\frac{a\xi}{2} = \frac{\xi(2-d)}{\mu^2} \int_0^\xi A^2\psi dx + \frac{\xi\varepsilon}{\mu^2} \int_0^\xi xA\left(A_{xx} - A\psi^2 + \frac{d-1}{x}A_x - \Delta A^3\right) dx \quad (4.7)$$

where both integrals converge as $\xi \to \infty$. Thus, we find the exact expression,

$$\mu^2 = \frac{2(2-d)}{a} \int_0^\infty A^2\psi dx + \frac{2\varepsilon}{a} \int_0^\infty xA\left(A_{xx} - A\psi^2 + \frac{d-1}{x}A_x - \Delta A^3\right) dx. \quad (4.8)$$

This is a regular perturbation of formulae for the NLS which are given in [24] [Section 8.1.3]. Once the structure of a solution is fixed the integrals can be determined. To obtain the result as stated in Propostion 3.3 we make *two* estimates of μ. One estimate follows from matching the solution in the region $\xi \gg 1, a\xi < 2$, on the lefthandside of the peak, to the solution for $a\xi \gg 1$. For this, we link a WKB estimate of the exponential decay rate of either the monotone solution or the multi-bump solution, for $\xi \gg 1, a\xi < 2$, to the slowly varying solution for $a\xi \gg 1$. The second estimate for μ follows from (global) estimates of both of the integral terms in (4.8). In order to do this we use approximations for the amplitude A which are derived in the next two Sections. In the case of a solution with one maximum, we find the ground state solution, see Section 5 and for the multi-bump solution we obtain a *sech* profile, see Section 6. In the latter case the quadratures can be evaluated exactly while the former requires numerical approximation.

4.4. Asymptotic analysis of the inner region. We consider next the general behaviour of the solutions when $a\xi$ is small; the inner region. This analysis is similar to that reported in [24, 15] and more relevant details are given there. Inspection of the equations (4.4) and (4.5) shows that if ε and $a\xi$ are both *small* then to leading order A and ψ satisfy the ordinary differential equations

$$A_{\xi\xi} = \psi^2 A - \frac{d-1}{\xi}A_\xi + A - A^3,$$

$$\psi_\xi = -2\psi\frac{A_\xi}{A} - \frac{d-1}{\xi}\psi.$$

From Lemma 4.1 we have that to leading order

$$\psi = -\frac{a\xi}{2} + \frac{1}{\xi A^2}\int_0^\xi (2-d)A^2\psi dx,$$

which validates the introduction of the rescaling $\psi = a\xi\phi$. Then the equation for A becomes

$$A_{\xi\xi} + \frac{d-1}{\xi}A_\xi - A + A^3 = a^2\xi^2\phi^2 A, \quad (4.9)$$

and Lemma 4.1 gives to leading order

$$\phi = -\frac{1}{2} - \frac{(d-2)}{\xi^2 A^2}\int_0^\xi A^2 x\phi dx.$$

Accordingly, if $a\xi \ll 1$, A will to leading order be given by a solution $R(\xi)$ of the *ground-state equation*

$$R_{\xi\xi} + \frac{d-1}{\xi}R_\xi + R^3 - R = 0, \qquad R'(0) = 0, \lim_{\xi\to\infty} R(\xi) = 0. \quad (4.10)$$

15

This equation has a discrete set of exponentially decaying solutions [16]: $R_0 \equiv 0$, the unique monotone solution R_1 (the ground state solution or Townes soliton) and an infinite sequence of non-monotone solutions R_K, with

$$R_K(\xi) = \frac{\nu_K}{\xi^{(d-1)/2}} e^{-\xi} \quad \text{as} \quad \xi \to \infty.$$

Note that the equation also admits exponentially growing solutions.

Starting with one of these solutions R_K it follows that, to leading order, ϕ satisfies the Volterra integral equation

$$\phi = -\frac{1}{2} - \frac{(d-2)}{\xi^2 R_K^2} \int_0^\xi R_K^2 x \phi dx.$$

We may generally solve this integral equation by using a Volterra series. In the limit of $d \to 2$ this gives

$$\phi = -\frac{1}{2} + \frac{(d-2)}{2\xi^2 R_K^2} \int_0^\xi R_K^2 x dx + \mathcal{O}((d-2)^2).$$

Note, that as R_K is exponentially decaying, all of the integrals in the Volterra series are rapidly convergent.

The amplitude A now is a perturbation of one of the solutions R_K of the ground state equation (4.10). Substituting the leading order expression $\psi = a\xi\phi$, where $\phi = \mathcal{O}(1)$, and $A = R_K$ into (4.4) it follows that the perturbation to (4.10) is of order $\mathcal{O}(a^2\xi^2) + \mathcal{O}(a\varepsilon)$. Therefore, the leading order expressions for A and ψ must be perturbed, these perturbations take a similar form as those described in [3], (see also [24]). If we set $A = R_K + B$ then, to leading order, the perturbation B evolves according to the expression

$$\mathcal{L}B \equiv B_{\xi\xi} + \frac{(d-1)}{\xi} B_\xi - B + 3R_K^2 B = \mathcal{O}(a^2\xi^2) + \mathcal{O}(a\varepsilon). \tag{4.11}$$

Therefore, we may develop a regular expansion for A of the form

$$A = R_K + a^2 A_1 + a\varepsilon A_2 + ... \tag{4.12}$$

where each of the terms A_i is exponentially decreasing. For $K = 1$ this is a natural perturbation of the ground state solution.

Significantly, this expansion for A is in general incomplete. For large ξ, the linear equation $\mathcal{L}B = 0$ has two linearly independent solutions, which are to leading order given by

$$\psi_1 = \xi^{-(d-1)/2} e^{-\xi} \quad \text{and} \quad \psi_2 = \xi^{-(d-1)/2} e^{\xi}.$$

The regular expansion (4.12) is sufficient as a perturbation of the ground state solution R_1, however, it excludes the contributions due to ψ_2 and these should not be ignored in general. Thus, a more general expression for the perturbation is obtained by adding the exponentially growing terms given by ψ_2. These terms become important when looking at a perturbation of the non-monotone solutions $R_K, K > 1$. Accordingly, following [3], we extend the expansion for the perturbation to give

$$A = R_K + a^2 A_1 + a\varepsilon A_2 + ... \frac{\alpha}{\xi^{(d-1)/2}} e^\xi \left(1 + a^2 B_1 + a\varepsilon B_2 + ..\right) \tag{4.13}$$

16

To ensure that the perturbation to the ground state solution R_K is small, we require in this expansion that α is an exponentially small term in a of the form $\alpha = e^{-\gamma/a}$. The terms $a^2\xi^2$ and αe^ξ then become significant when $a\xi$ is of order one.

5. The monotone solution. First, we focus on constructing the monotone solutions Q_1 on the $k = 1$ solution branch. We expect these solutions to have the form of the regular perturbation to the monotone solution $R_1(\xi)$ described in (4.12). Since there exist no further maxima, apart from the one in $\xi = 0$, the solutions do not contribute to the leading order for $\xi \gg 1$ (far-field profile). Substituting the expressions (4.12) and $\psi = a\xi\phi$ into (4.8) we have to leading order

$$
\mu^2 = 2(2 - d) \int_0^\infty R_1^2 \phi x \ \left(1 + \mathcal{O}(a^2, a\varepsilon)\right) \ dx
$$
$$
+ \frac{2\varepsilon}{a} \int_0^\infty x R_1 \left(R_{1,xx} - R_1 a^2 x^2 \phi^2 + \frac{d-1}{x} R_{1,x} - \Delta R_1^3 \right) \left(1 + \mathcal{O}(a^2, a\varepsilon)\right) \ dx.
$$
(5.1)

Each of these integrals can be estimated in turn, where semi-explicit expressions are possible in the limit of $d \to 2$ and numerical expressions otherwise. In particular for $d - 2$ small

$$
\int_0^\infty R_1^2 \phi x \, dx \approx -\frac{1}{2} \int_0^\infty R_1^2 x \, dx + \mathcal{O}(d - 2),
$$

since $\phi = -\frac{1}{2} + \mathcal{O}(d - 2)$, where the remainder term in this expression depends on $(d - 2)$ but does not depend upon a or ε. Likewise, the contribution to the second integral in (5.1) is also dominated by the ground state profile and

$$
\int_0^\infty x R_1 \left(R_{1,xx} - a^2 \phi^2 R_1 x^2 + \frac{d-1}{x} R_{1,x} \right) dx \approx
$$
$$
\int_0^\infty x R_1^2 (1 - R_1^2) \left(1 + \mathcal{O}(a^2(d - 2))\right) \ dx
$$

since R_1 satisfies equation (4.10). Hence

$$
\mu^2 = (d - 2) \left(\int_0^\infty x R_1^2 \, dx + \mathcal{O}\left((d - 2), a^2, a\varepsilon\right) \right)
$$
$$
+ \frac{2\varepsilon}{a} \left(\int_0^\infty x R_1^2 (1 - (1 + \Delta)R_1^2) \, dx + \mathcal{O}\left(a^2, a\varepsilon\right) \right).
$$
(5.2)

5.1. The matching for the monotonically decreasing solution. To leading order, the behaviour of the function A at large values of ξ for the CGL is identical to that for the monotone solution of the NLS described in [24]. In particular, the matching between the exponentially decaying solution for $a\xi < 2$ and the polynomially decaying solution for $a\xi > 2$ is identical. Following [24], we have that in this case, a solution which is a perturbation of $R_1(\xi)$ evolves smoothly into one of the form μ/ξ with the matching constant

$$
\mu^2 = 2\nu_1^2 \frac{e^{-\pi/2a}}{a}.
$$
(5.3)

17

Substituting into (5.2) we obtain

$$2\nu_1^2 \frac{e^{-\pi/2a}}{a} = \left((d-2)M_1 + \frac{2\varepsilon}{a}(M_1 - (1+\Delta)M_2)\right)\left(1 + \mathcal{O}\left(a^2, a\varepsilon, (d-2)^2\right)\right) \quad (5.4)$$

where

$$M_1 = \int_0^\infty xS^2(x)\, dx \approx 1.862 \quad \text{and} \quad M_2 = \int_0^\infty xS^4(x)\, dx \approx 3.725.$$

Rearranging, this gives the asymptotic expression (3.8) in Proposition 3.3.

Here S is the monotone solution of the ground state equation (4.10) with $d = 2$ and the integrals are evaluated by numerical quadrature. It can be shown [11] that $2M_1 = M_2$ for $d = 2$. The constant ν_1 is a related to the matching of the exponential and algebraically decaying solutions [24] and we have from numerical quadrature that when $d = 2$

$$\nu_1 = \lim_{x\to\infty} x^{(d-1)/2} e^x S(x) \approx 3.150.$$

Critically, this gives a condition on the relationship between ε and δ for which the monotonically decreasing solutions Q_1 may exist and we require

$$(d-2)M_1 + \frac{2\varepsilon}{a}(M_1 - (1+\Delta)M_2) > 0.$$

In the limit case $d = 2$ [11], this implies that $\varepsilon(1+2\Delta) = \varepsilon + 2\delta < 0$ must be satisfied, recovering exactly the result in [10] where modulational analysis is used to determine the stability of monotonically decreasing blow-up profiles. Their instability result relies on exactly the same comparison of integrals, [11, 10]. For $d - 2 > 0$ and small we see existence over a wider range of ε and δ. In particular, for $\delta = 0$ (hence $\Delta = 0$) there exists a solution for a small (the branch a_-) with

$$\varepsilon \sim \frac{(d-2)a_-}{2}.$$

For more general values of d we must evaluate expressions for R_1, ϕ and the integrals in (5.1) by numerical methods. In particular, if $d = 3$, $\nu_1 \approx 2.713$,

$$\int_0^\infty xR_1^2\, dx \approx 2.580 \quad \text{and} \quad \int_0^\infty xR_1^4\, dx \approx 18.813.$$

This leads to the expression (3.8) with $C_1 \approx 0.1753$, $C_2 \approx 2.205$ and $C_3 \approx 0.1359$. Similar calculations may be performed for any dimension.

6. Asymptotic analysis of the multi-bump solutions.

6.1. Overview. We now consider the possible multi-bump solutions that were observed in the numerical calculations presented here and in [19]. In the analysis for the inner solution (the solution for $a\xi$ small) in section 4.4, we identified the possibility of having exponentially growing perturbations of the solutions of the ground state equation (4.13). This result was obtained by studying (4.11). We find that in the region where $\xi = \mathcal{O}(1/a)$ the perturbation $a^2\xi^2$ in (4.11) to the ground state equation has the same order as the other terms. And, there is a large perturbation of the

18

solution from $R_K(\xi)$ as the terms αe^ξ become significant. It is precisely in this range of $\xi = \mathcal{O}(1/a)$ that we observe, in numerical simulations, the existence of additional peaks of order one. When a is small, we are able to give a precise description of these peaks in the following two cases: the case of $d - 2$ *small*, (indeed exponentially small in a), and the case of general d but with ε small (ε proportional to a). When *either* of these conditions is satisfied we are able to give a complete description of the bifurcation diagram.

We shall concentrate our analysis only on solutions with two maxima on the interval $\xi \in (-\infty, \infty)$. This is due the numerical ODE computations reported in [19] suggesting that only the single and two-bump solutions are stable. We have also seen numerically that the higher multi-bump solutions are unstable through both PDE and ODE compuations. As such we leave their further investigation for a future time.

6.2. The form of the peaks. The numerical evidence presented in Figure 3.2, indicates that the peaks of the function $|Q|$ are asymptotically located at the points κ/a, with $\kappa = 1$. Also, the solution $|Q|$ takes on a localised form that is independent of a, provided that ε is small. We follow the asymptotic analysis of [3] and assume that the multi-bumps are found in the region where $\xi = \mathcal{O}(\frac{1}{a})$. Here the peaks strongly resemble a localized solution of the one-dimensional focussing NLS equation. We assume that the peak is located at the point

$$\xi^* = \kappa/a$$

and seek to determine κ. In order to do this we rescale the Q-equation (2.6) by setting

$$\xi = \frac{\kappa}{a} + s \tag{6.1}$$

and consider an expansion of the solution in terms of a with $a \ll 1$. From this an expression for κ will be obtained.

Substituting (6.1) into (2.6) leads to

$$Q_{ss} + i\kappa Q_s - Q + |Q|^2 Q = i\varepsilon Q_{ss} - a\frac{(d-1)}{\kappa + as}Q_s - ia(sQ)_s - i\Delta\varepsilon|Q|^2 Q + \mathcal{O}(a\varepsilon). \tag{6.2}$$

We now express $Q(s)$, in the neighbourhood of $s = 0$, as an asymptotic series in a

$$Q(s) = Q_0(s) + aQ_1(s) + o(a). \tag{6.3}$$

This gives the following reduced equation for Q_0

$$Q_{0,ss} + i\kappa Q_{0,s} - Q_0 + |Q_0|^2 Q_0 = 0. \tag{6.4}$$

We now rescale the phase of Q_0 in (6.4) by setting

$$Q_0(s) = e^{-\frac{i\kappa s}{2}} S_0(s) \tag{6.5}$$

which leads to

$$S_{0,ss} - \left(1 - \frac{\kappa^2}{4}\right) S_0 + |S_0|^2 S_0 = 0. \tag{6.6}$$

19

Without loss of generality we may assume the solution of (6.6) to be real, so that up to an arbitrary multiplicative constant of modulus one, we have

$$S_0(s) = \sqrt{2\left(1 - \frac{\kappa^2}{4}\right)} \operatorname{sech}\left(\sqrt{1 - \frac{\kappa^2}{4}}\, s\right). \qquad (6.7)$$

Observe that this solution is valid provided that we are in the region $\kappa < 2$ (i.e. $\xi < 2/a$). Note further that the form of S_0 is independent of a. Important for the matching later on is that for $|s|$ large and a small, this solution is exponentially decaying. From (6.5) it also follows that the gradient of the phase ψ is $-\frac{\kappa}{2}$ to leading order.

6.3. Locating the peaks. The terms on the righthandside of (6.2) are of the same order when ε and a are of the same order and, therefore, we set $\varepsilon = Ka$ and estimate the value of K. Consider now the equation for Q_1. The values of κ and K are fixed by the compatibility condition and thus in the asymptotic series, the term $a|Q_1|$ is small in comparison to $|Q_0|$. Taking the terms of $\mathcal{O}(a)$ together gives the following equation for Q_1

$$Q_{1,ss} + i\kappa Q_{1,s} - Q_1 + Q_0^2 \bar{Q}_1 + 2|Q_0|^2 Q_1 =$$
$$iKQ_{0,ss} + \frac{(1-d)}{\kappa} Q_{0,s} - i(sQ_0)_s - i\Delta K|Q_0|^2 Q_0. \qquad (6.8)$$

Again, we rescale the phase by setting

$$Q_1(s) = e^{-\frac{i\kappa s}{2}} S_1(s) \qquad (6.9)$$

then, using (6.5), we obtain

$$S_{1,ss} - \left(1 - \frac{\kappa^2}{4}\right) S_1 + S_0^2 \bar{S}_1 + 2|S_0|^2 S_1 = iK\left(-\frac{\kappa^2}{4} S_0 - i\kappa S_{0,s} + S_{0,ss}\right)$$
$$+ \left(\frac{(1-d)}{\kappa} - is\right)\left(-\frac{i\kappa}{2} S_0 + S_{0,s}\right) - iS_0 - i\Delta K S_0^3. \qquad (6.10)$$

Setting $S_1 = t + iv$ and splitting into real and complex parts leads to (since S_0 is real)

$$t_{ss} - \left(1 - \frac{\kappa^2}{4}\right) t + 3t S_0^2 = K\kappa S_{0,s} + \frac{1-d}{\kappa} S_{0,s} - \frac{\kappa s}{2} S_0 =: f \qquad (6.11)$$

and

$$v_{ss} - \left(1 - \frac{\kappa^2}{4}\right) v + v S_0^2 = K\left(\kappa S_{0,ss} - \frac{\kappa^2}{4} S_0\right) + \frac{d-3}{2} S_0 - s S_{0,s} - \Delta K S_0^3 =: g. \qquad (6.12)$$

For the asymptotic expansion to be consistent we require

$$t(0) = v(0) = 0, \quad \text{and} \quad |t| \to 0, |v| \to 0 \quad \text{as} \quad |s| \to \infty.$$

We will determine the form of t and v by using the variation of constants formula. For subsequent use, we define the right-hand side of (6.11) to be the function f and the

20

right-hand side of (6.12) to be the function g. First, we focus on the equation for t and more specifically on the homogeneous part of (6.11). A solution to this homogeneous equation is $\psi_1(s) = S_{0,s}(s)$ (which is odd and exponentially decaying). Also, there exists an exponentially growing, even valued solution ψ_2 that is linearly independent of $\psi_1(s)$; $\psi_1(s)$ and $\psi_2(s)$ have a constant Wronskian W_1. Computing directly,

$$\psi_2(s) = S_{0,s} \int_0^s \frac{dy}{S_{0,y}^2(y)} \sim \exp\left(\sqrt{1 - \frac{\kappa^2}{4}} s\right) \quad \text{for large } s. \tag{6.13}$$

It follows by the variation of constants, using $t(0) = 0$, that

$$t(s) = A_1 \psi_2(s) + \psi_1 \int_0^s \frac{\psi_2 f}{W_1} dz - \psi_2 \int_0^s \frac{\psi_1 f}{W_1} dz \tag{6.14}$$

where A_1 is arbitrary. Then using the fact that ψ_1 decays exponentially we find that

$$t(s) \to \left(A_1 - \frac{I_1}{W_1}\right) \psi_2(s) \quad \text{as} \quad s \to \infty \tag{6.15}$$

$$t(s) \to \left(A_1 + \frac{I_1}{W_1}\right) \psi_2(s) \quad \text{as} \quad s \to -\infty \tag{6.16}$$

where I_1 is defined as

$$I_1 = \int_0^\infty f\psi_1 ds = \int_0^\infty \left(K\kappa S_{0,s} + \frac{1-d}{\kappa} S_{0,s} - \frac{\kappa s}{2} S_0\right) S_{0,s} ds. \tag{6.17}$$

Now, we study v and we find that $\phi_1 = S_0$ is a solution of the homogeneous part of equation (6.12). Again, ϕ_1 is exponentially decaying and odd. There also exists a second linearly independent, exponentially growing, even valued solution

$$\phi_2 = S_0 \int_0^s \frac{dy}{S_0^2(y)},$$

and, ϕ_1 and ϕ_2 have a constant Wronskian W_2. In a similar way as before, using $v(0) = 0$, it follows that

$$v(s) = A_2 \phi_2(s) + \phi_1 \int_0^s \frac{\phi_2 g}{W_2} dz - \phi_2 \int_0^s \frac{\phi_1 g}{W_2} dz$$

where A_2 is a constant. Then

$$v(s) \to \left(A_2 - \frac{I_2}{W_2}\right) \phi_2(s) \quad \text{as} \quad s \to \infty \tag{6.18}$$

$$v(s) \to \left(A_2 + \frac{I_2}{W_2}\right) \phi_2(s) \quad \text{as} \quad s \to -\infty \tag{6.19}$$

where

$$I_2 = \int_0^\infty g\phi_1 ds = \int_0^\infty \left(K\left(\kappa S_{0,ss} - \frac{\kappa^2}{4} S_0\right) + \frac{d-3}{2} S_0 - s S_{0,s} - K\Delta S_0^3\right) S_0 ds. \tag{6.20}$$

21

First, we focus on those solutions with one maximum in the region $\xi = \mathcal{O}(\frac{\kappa}{a})$. These solutions decay exponentially away from $s = 0$ and therefore, cannot have an exponential growth in $t(s)$ and $v(s)$ for $s \to \infty$ and for $s \to -\infty$. Thus, it follows from (6.15), (6.16), (6.18) and (6.19), since ψ_2 and ϕ_2 are both exponentially growing, that $A_1 = 0$, $I_1 = 0$, $A_2 = 0$ and $I_2 = 0$. Substituting the expression for S_0 (6.7) into I_1 and I_2 and using of the exact integrals

$$\int_0^\infty (S_{0,s})^2 ds = \frac{2}{3} \left(\sqrt{1 - \frac{\kappa^2}{4}} \right)^3 , \int_0^\infty s S_0 S_{0,s} ds = -\sqrt{1 - \frac{\kappa^2}{4}},$$

$$\int_0^\infty S_0 S_{0,ss} ds = -\frac{2}{3} \left(\sqrt{1 - \frac{\kappa^2}{4}} \right)^3 , \int_0^\infty S_0^2 ds = 2\sqrt{1 - \frac{\kappa^2}{4}}, \tag{6.21}$$

$$\text{and } \int_0^\infty S_0^4 ds = \frac{8}{3} \left(\sqrt{1 - \frac{\kappa^2}{4}} \right)^3 ,$$

leads to

$$I_1 = \frac{1}{2\kappa} \sqrt{1 - \frac{\kappa^2}{4}} \left[\frac{4}{3} \left(1 - \frac{\kappa^2}{4} \right) (K\kappa^2 + 1 - d) + \kappa^2 \right] \tag{6.22}$$

and

$$I_2 = \sqrt{1 - \frac{\kappa^2}{4}} \left[-\frac{2}{3} K\kappa \left(1 - \frac{\kappa^2}{4} + \frac{3\kappa}{4} \right) + d - 2 - \frac{8}{3} \Delta K \left(1 - \frac{\kappa^2}{4} \right) \right]. \tag{6.23}$$

A relationship between the values of κ, K and Δ then follows from the two conditions

$$I_1 = 0 \quad \text{and} \quad I_2 = 0. \tag{6.24}$$

We consider first the case of $\delta = 0$ hence $\Delta = 0$. In this case there is precisely one exact solution of (6.24) with $0 < \kappa < 2$ which is given by

$$\kappa = 1 \quad \text{and} \quad K = d - 2. \tag{6.25}$$

Therefore, we find that

$$\varepsilon = (d - 2)a, \quad \xi_{max} = \frac{1}{a} + hot. \tag{6.26}$$

(*hot* denotes higher order terms.) A key result of this calculation is that the location of the peak depends upon a but not explicitly upon d. Indeed, in the limit of $d = 2$ we still have $\kappa = 1$. The dominant contribution to the function $A = |Q|$ in the global identity (4.8) thus comes from the localised peak, centred at $1/a$ for which both the functional form and the form of the phase ψ are as given in Section 6.2. The integrals in (4.8) can thus be evaluated explicitly.

It also follows from the above expression, that in the limit of $d = 2$ we find that $\varepsilon = 0$ to leading order in a. In fact we see presently that as $d \to 2$, both ε and $d - 2$ are exponentially small functions of a, which is consistent with the above estimate.

Now we consider $\delta \neq 0$ (hence $\Delta \neq 0$) and $\varepsilon = 0$. Setting $\varepsilon = 0$ would imply that $K = 0$, however, if we first substitute $\Delta = \frac{\delta}{aK}$ where $\delta \neq 0$ and then set $K = 0$, we find that

$$\delta = a\frac{d^2 - 4}{8}, \qquad \kappa = 2\sqrt{\frac{d-1}{d+2}}$$

Similar to the above calculation, we obtain that $\kappa \to 1$ and $\delta \to 0$ as $d \to 2$.

Additional solutions for general δ may also be found, but we will concentrate on the case $\delta = 0$ for comparison with numerics.

6.4. Evaluating the integrals in the identity (4.8). So far, we studied the structure of the multi-bump solutions in different regions of ξ. As a final step in constructing these solutions, we determine the integrals in equation (4.8). We obtain the condition on a, d, ε and δ under which they exist as stated in the in Proposition 3.3. For this we use the asymptotic solution determined in the previous section. The key result we exploit here is that, for small a, the solution has a peak at $1/a$, to leading order, independent of the value of d. Thus, we study the solution with a single peak at $\xi = \frac{1}{a} + hot$ over a range of values of d; we construct the $k = 2$ solution. This solution will be estimated on different ranges of ξ. To evaluate the integrals in (4.8), we split both integrals into three parts from 0 to ξ_1 to ξ_2 to ∞ where $1 \ll \xi_1 \ll \frac{1}{a} \ll \xi_2$. On each of these three regions the solution is known from previous sections to leading order and the integrals can be estimated.

When integrating from 0 to ξ_1, in other words, $x \ll \frac{1}{a}$, $A(x)$ is either exponentially small or $A(x) \approx R_K$ and $\psi = -\frac{ax}{2}$. The contribution over this region to the first integral in (4.8) is therefore smaller than

$$-a \int_0^\infty R_K^2 x \, dx = \mathcal{O}(a).$$

In a similar way, the contribution to the second integral in this regions is either exponentially small (in the case that A is exponentially small) or it is $\mathcal{O}(1)$ when $A \approx R_K$.

Now we focus on the integrals in (4.8) in the range where $x > \xi_2 \gg \frac{1}{a}$. We find by using (4.3) that $A^2\psi = -\frac{\mu^2}{ax^3}$ to leading order so that the contribution to the first integral in (4.8) over this range is of order a. Similarly, we find that

$$xA\left(A_{xx} - A\psi^2 + \frac{d-1}{x}A_x - \Delta A^3\right) \approx -\frac{\mu^2}{x^3}\left(\frac{1}{a^2} + d - 3 - \Delta\mu^2\right)$$

so that the contribution to the second integral is to leading order given by $-\frac{\mu^2}{8}$.

Finally, in the middle range of ξ values, in the neighbourhood of $\frac{1}{a}$, here $\xi_1 < x < \xi_2$, we know from Section 6.2 that A and ψ are to leading order given by

$$S(x) = \sqrt{2\left(1 - \frac{\kappa^2}{4}\right)}\,\text{sech}\left(\sqrt{1 - \frac{\kappa^2}{4}}\left(x - \frac{\kappa}{a}\right)\right) \quad \text{and} \quad \psi = -\frac{\kappa}{2}. \tag{6.27}$$

Therefore, in this region the contribution to the first integral is to leading order given

23

by

$$-\int_{\xi_1}^{\xi_2} \kappa \left(1 - \frac{\kappa^2}{4}\right) \operatorname{sech}^2\left(\sqrt{1 - \frac{\kappa^2}{4}}\left(x - \frac{\kappa}{a}\right)\right) dx$$

$$= -\kappa \left(1 - \frac{\kappa^2}{4}\right) \int_{-\infty}^{\infty} \operatorname{sech}^2\left(\sqrt{1 - \frac{\kappa^2}{4}}y\right) dy + hot$$

$$= -2\kappa \sqrt{1 - \frac{\kappa^2}{4}} + hot$$

where the first equality is obtained by introducing the rescaled variable $y = x - \frac{\kappa}{a}$ and using the fact that $a \ll 1$.

The contribution to the second integral in (4.8) for $\xi_1 < x < \xi_2$ is given to leading order given by

$$\int_{\xi_1}^{\xi_2} xS \left(S_{xx} - S\psi^2 + \frac{d-1}{x}S_x - \Delta S^3\right) dx$$

$$= \int_{-\infty}^{\infty} \left(y + \frac{\kappa}{a}\right) S \left(S_{yy} - S\psi^2 + \frac{d-1}{y + \frac{\kappa}{a}}S_y - \Delta S^3\right) dy + hot$$

$$= \int_{-\infty}^{\infty} \frac{\kappa}{a} S \left(S_{yy} - S\psi^2 - \Delta S^3\right) dy$$

$$= -\frac{\kappa}{a} \int_{-\infty}^{\infty} \left((S_y)^2 + S^2\psi^2 + \Delta S^4\right) dy$$

$$= -\frac{2\kappa}{3a}\sqrt{1 - \frac{\kappa^2}{4}} \left(2 + \kappa^2 + 8\Delta(1 - \frac{\kappa^2}{4})\right).$$

where A is given by (6.27). A similar error analysis to the previous case implies that the error in the above integral when extended to the real line is $\mathcal{O}(1)$ as $a \to 0$.

Summarizing, the two integrals in (4.8) when integrated from 0 to ∞ are given to leading order by

$$\int_0^{\infty} A^2 \psi dx = -2\kappa\sqrt{1 - \frac{\kappa^2}{4}},$$

and

$$\int_0^{\infty} xA \left(A_{xx} - A\psi^2 + \frac{d-1}{x}A_x - \Delta A^3\right) dx =$$

$$-\frac{2\kappa}{3a}\sqrt{1 - \frac{\kappa^2}{4}} \left(2 + \kappa^2 + 8\Delta(1 - \frac{\kappa^2}{4})\right).$$

Substituting these expressions for the integrals into (4.8) and including the error terms gives

$$\mu^2 = \left[-\frac{4\kappa}{a}\sqrt{1 - \frac{\kappa^2}{4}}\left(2 - d + \frac{\varepsilon}{3a}(2 + \kappa^2) + \Delta\varepsilon\frac{8}{3a}\left(1 - \frac{\kappa^2}{4}\right)\right)\right](1 + \mathcal{O}(a)). \quad (6.28)$$

To complete the matching we estimate the value for the parameter μ. This is done by matching the exponentially decaying behaviour to the right and away from the main

24

peak of the solution to the polynomially decaying behaviour in the tail. The analysis is, to leading order, identical to the NLS calculation for the multi-bump solutions and it is based on the WKB approximation that was described in [3]. We obtain that

$$\mu^2 = \frac{16\kappa(1 - \kappa^2/4)^{3/2}}{a^2} e^{-\lambda_2/a}, \quad \lambda_2 = \pi - 2\sin^{-1}(\kappa/2) - \kappa\sqrt{1 - \kappa^2/4}, \qquad (6.29)$$

so that if $\kappa = 1$ (as in the case of $\delta = 0$) we find that

$$\mu^2 = \frac{6\sqrt{3}}{a^2} e^{-(2\pi/3 - \sqrt{3}/2)}.$$

The value of κ in general follows by imposing both conditions in (6.24).

We now substitute (6.29) into the expression (6.28) to determine a condition relating κ, K and Δ. On rearranging we obtain

$$(4 - \kappa^2)e^{-\lambda_2/a} = \left((d-2)a - \frac{\varepsilon}{3}(2 + \kappa^2) - \frac{8}{3}a\Delta\varepsilon \left(1 - \frac{\kappa^2}{4}\right)\right)(1 + \mathcal{O}(a)). \quad (6.30)$$

In general, this expression is complicated since there is a subtle relationship between d, κ, ε and Δ, although in all cases $\kappa \to 1$ as $d \to 2$. In the case of $\delta = 0$ ($\Delta = 0$ and $\kappa = 1$), (6.30) reduces to

$$3e^{-\lambda_2/a} \sim (d-2)a - \varepsilon, \quad \lambda_2 = 2\pi/3 - \sqrt{3}/2. \qquad (6.31)$$

We observe that the values of $\kappa = 1$, $\varepsilon = a(d-2)$ that were obtained in Section 6.3 by the use of the Fredholm alternative, set the right hand side of (6.31) identically to zero. This is consistent with the exponentially small estimate of μ when a is small. However, the value of the Fredholm alternative calculation in finding the location ($\xi = \frac{1}{a}$) and form of the peak is plain, as when combined with the global estimate we not only recover the earlier condition linking a and ε but also find the exponential link between a and $d - 2$ in the limit of $d \to 2$ and $a \to 0$.

7. Numerical results. In this Section, we consider two numerical simulations. Firstly, we look at numerical solutions of the ordinary differential equation (2.6) that must be satisfied by the self-similar solutions. These numerics are compared to the asymptotic formulae computed in the previous sections. It should be noted that the existence of solutions to this ODE does not in any way guarantee the formation of blow-up solutions to the full CGL for a broad class of initial data. Therefore, we also solve the PDE problem (1.1) directly.

7.1. Solution of the ordinary differential equation. In order to find solutions of the ODE (2.6) a parameter continuation with respect to ε was performed with the (collocation based) two-point boundary value solver and path following algorithms in the package AUTO [9]. This package requires a good initial guess for the solution at a certain value of ε. This initial solution was computed with a shooting algorithm combining the ODE solver DOP853 [12] and the nonlinear solver DNSQE [20]. In light of the prediction for the location (6.26) of the maximum of the non-monotone profile with two bumps on the real line ($k = 2$), the boundary value problem (2.6) was solved with the normalization and symmetry conditions (3.1) enforced at the

25

origin and the slow-growth condition (3.3) enforced at finite $L = 1000$. From (6.26), $\xi_{max} = \frac{1}{a} + hot$, this means that we should be able to continue the $k = 2$ solution branch until $a \sim 10^{-3}$. The bifurcation diagram in the (a, ε)-plane where solutions with two maxima exist as computed in this manner is shown in Figure 3.1 and the structure of the solution as moving along the branch in the (a, ε)-plane is given in Figure 3.2.

The ODE computation that really motivated us to solve the PDE directly is given in Figure 1.1. Here we see the remarkable feature that the range of ε for which multi-bump solutions exist, is larger than that for the monotone solutions! This begs the question of whether or not multi-bump solutions in this regime are stable. In [19], the authors considered this question by numerically examining the spectrum of the linearization about the computed solutions and found that the lower part of the branch of $k = 2$ solutions is linearly stable for ε sufficiently small. This in contrast to the monotone solutions that are found to be stable on the upper part of the $k = 1$ branch. We now consider computations of the solutions of the full PDE to examine the stability of the solutions and to see which initial data converge to the various types of stable self-similar blow-up profiles.

7.2. Solution of the partial differential equation. The numerical approximation of the large solutions of the full PDE (1.1), which evolve over small length and time scales, requires the use of an adaptive method. To ensure spatially accurate final-time profiles we use the scale-invariant moving mesh PDE approach [13] that has previously been used in the study of blow-up problems of this type [5, 4]. In this semi-discretization method, a set of computational nodes are distributed in a finite spatial interval and the spatial derivatives of the PDE are discretised by using a collocation method. Then, the resulting system of ordinary differential equations is solved by using a stiff ODE solver. To ensure a correct resolution of the singularity, the computational nodes are moved to *equidistribute* the integral of a user-defined quantity, a *monitor function*, between mesh points. We use the *scale-invariant monitor function*

$$M = |\Psi|^2$$

so that the blow-up solutions are resolved at all times. This was effective for the computations of NLS reported in [4] and it has the property that it admits moving meshes which move nodes along level sets of the similarity variables defined in (2.2). Since the symmetries of the CGL are the same as for the NLS, a similar method is expected to work well in this case. We take a slightly different approach from the dynamic rescaling method described in [24, 15], as we are not assuming any particular relation between the solution magnitude and the spatial and temporal scales on which the solution is evolving. Instead we follow any emergent scaling in the problem.

In Figure 7.1, we consider a numerical simulation of the full PDE starting with a non-monotone initial condition for $d = 3$ and $\varepsilon = 0.2$. This value of ε is chosen such that it lies beyond the range of existence of the monotone solutions. The resulting calculation, presented in the rescaled coordinates, show a stabilization of the blow-up solution to a multi-bump profile ($k = 2$).

The history of the numerical investigation of blow-up phenomena is plagued with errors and false-starts. We have confidence in the methods used here because they give results consistent with asymptotics and numerically computed ODE profiles. However, that might not be enough for the skeptical reader. The reliability of these methods comes from the fact that they can, under appropriate assumptions, lead

26
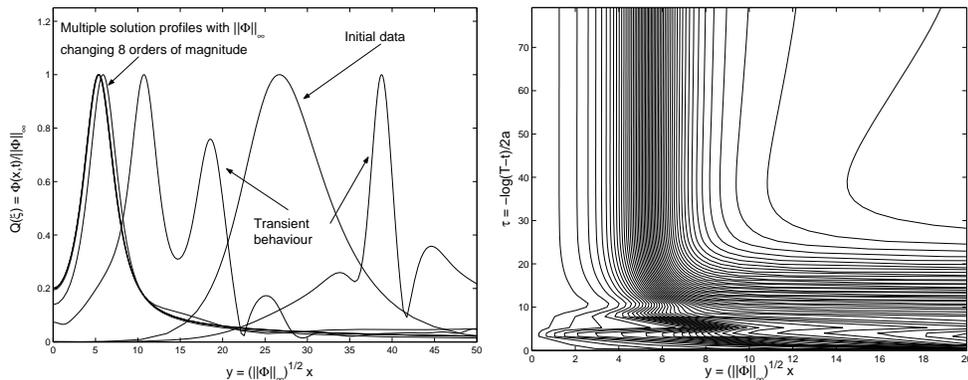
FIG. 7.1. *(left) Convergence of a non-monotone initial condition to a multi-bump similarity solution in the rescaled dynamical coordinates. (right) The grid lines of the moving mesh method plotted in the rescaled dynamical coordinates. After an initial transient phase, they are essentially constant in the region of the peak.*

to uniform error estimates [6]. This is because of the special scaling structure of the monitor function used. As an extra consequence, the dynamic grid follows level sets of any emergent similarity variable. Hence, the computational variables can be thought of as mimicking the similarity variables. This can be seen in Figure 7.1(right) where, after an initial transient phase, the grid lines are essentially constant in the rescaled variables.

To demonstrate the stability of various solutions on the $k = 1$ and $k = 2$ solution branches, we now consider four cases with fixed $d = 3$. With both monotone and non-monotone initial data we take $\varepsilon = 0.1 < \varepsilon_1^* < \varepsilon_2^*$ and $\varepsilon_1^* < \varepsilon = 0.22 < \varepsilon_2^*$ (recall that at $\varepsilon_{1,2}^*$ the fold bifurcation takes place and the $k = 1, 2$ solutions cease to exist). The data from each case is presented in Figure 7.2. For monotone initial data no blow-up is observed when $\varepsilon = 0.22$, Figure 7.2b; the evolution of the profile is presented in physical coordinates. All the other cases are presented in the rescaled coordinates (2.2). For comparison, the ODE solutions found for the same value of ε on both the upper and the lower part of the solution branches is also indicated. We see that the ODE solution found on the lower part of the $k = 2$ solution branch and the final profile at $t = T^-$ coincide and, hence, in agreement with the ODE numerics in [19], the lower part of the $k = 2$ solution branch is stable.

Additional computations lead us to speculate the following.

CONJECTURE 1. *i) For $0 < \varepsilon < \varepsilon_1^*$ there exists a wide class of initial data such that the solutions on the upper part of the $k = 1$ (monotone) solution branch are stable. For $\varepsilon > \varepsilon_1^*$ there are no stable monotone blow-up solutions.*
ii) For $0 < \varepsilon < \varepsilon_2^*$ there exists a wide class of initial data such that the lower part of the $k = 2$ solution branch is stable. For $\varepsilon > \varepsilon_2^*$ there are no stable $2-$bump solutions.

To summarise, we have not only found stable non-monotone profiles but we have also found them to exist in a broader region of parameter space than the monotone ones. This is in complete contrast to other blow-up problems; for most blow-up problems the pattern of minimal shape is the only stable one.

27
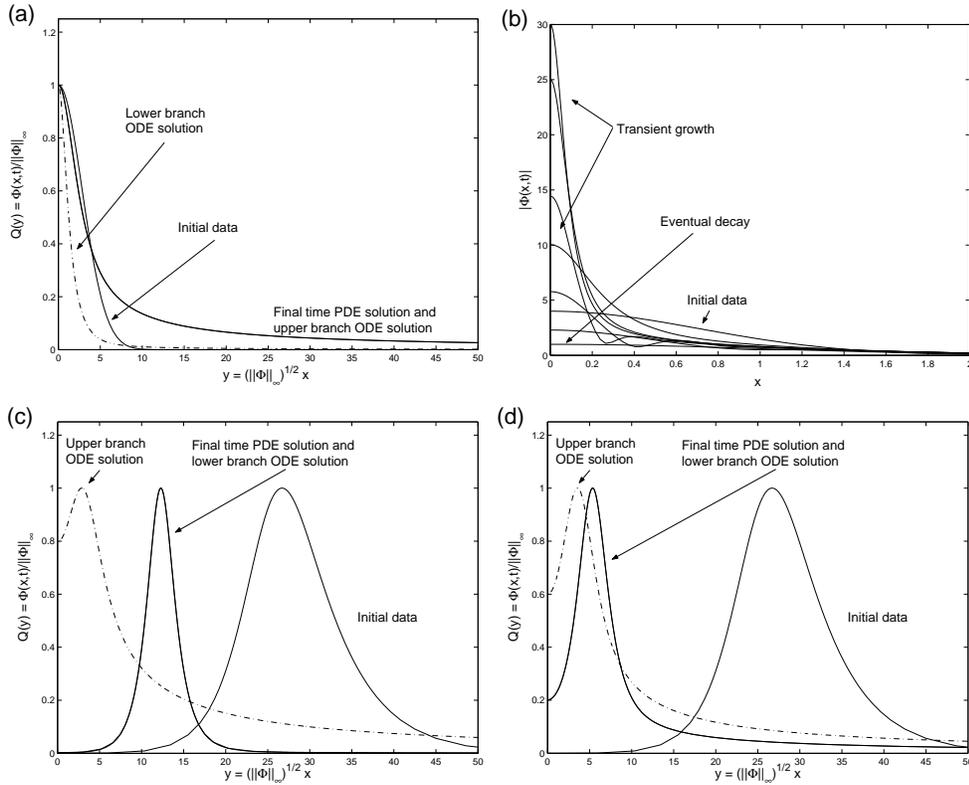
Fig. 7.2. *Numerical simulations of the full CGL for monotone and non-monotone initial conditions. The initial solution, $t = t_0$, is given, as well as the final-time profile and the ODE solutions that were observed for the same ε on both the upper and the lower part of the $k = 1$, resp $k = 2$, solution branch are given. In all but one case, the profiles are presented in rescaled coordinates. As indicated in Figure 7.1 the transient dynamics can be quite complicated and have been omitted for clarity. (a) Monotone initial data where $\varepsilon = 0.1 < \varepsilon_1^* < \varepsilon_2^*$ converge to a monotone final profile found on the upper part of the $k = 1$ solution branch. (b) Monotone initial data, plotted in the physical coordinates, decay to the zero solution for $\varepsilon_1^* < \varepsilon = 0.22 < \varepsilon_2^*$. (c) Non-monotone initial data, where $\varepsilon = 0.1 < \varepsilon_1^* < \varepsilon_2^*$, converge to a non-monotone final time profile found on the lower part of the $k = 2$ branch. (d) Non-monotone initial data, where $\varepsilon_1^* < \varepsilon = 0.22 < \varepsilon_2^*$, also converge to a non-monotone final time profile found on the lower part of the $k = 2$ branch.*

It would be very interesting indeed to extend to the $k-$bump solutions for $k > 2$. We have not included our numerics on these solutions here because they indicate, in agreement with results in [19], that these are unstable. However, in principle they could be constructed asymptotically as we described in the previous sections. It would, however, be most intriguingly to try and answer the question what $\sup_n \varepsilon_n^*$ is, if it exists at all. This is still an open problem.

REFERENCES

[1] I.S. Aranson and L. Kramer, *The world of the complex Ginzburg-Landau equation*, Rev. Mod. Phys. **74** (2002), 99–143.

[2] H.R. Brand, P.S. Lomdahl and A.C. Newell, *Benjamir-Feir turbulence in convective binary fluid mixtures*, Physica D **23** (1986) 345–362.

[3] C.J. Budd, *Asymptotics of multi-bump blow-up self-similar solutions of the nonlinear Schrödinger equation*, SIAM J. Appl. Math. **62** (2002), no. 3, 801–830.

[4] C.J. Budd, S. Chen, and R.D. Russell, *New self-similar solutions of the nonlinear Schrödinger equation with moving mesh computations*, J. Comp. Phys. (1999), 756–789.

[5] C.J. Budd, W. Huang, and R. Russell, *Moving mesh methods for problems with blow-up*, SIAM J. Sci. Comp. **17** (1996), 305–327.

[6] C.J. Budd, R.D. Russell, and J.F. Williams, *Optimal grids and uniform error estimates for PDEs with blow-up*, In preparation, 2004.

[7] A. Davey, L.M. Hocking and K. Stewartson, *On the nonlinear evolution of three-dimensional disturbances in plane Poiseuille flow*, J. Fluid Mech. **63** (1974) 529–536.

[8] R.C. DiPrima and H.L. Swinney, *Instabilities and transition in flow between concentric cylinders*, in Hydrodynamic Instabilities and the Transition to Turbulence (H. Swinney, J. Gollub eds.), *Topics in Applied Physics 45* (1981) Springer Verlag, New York.

[9] E. J. Doedel, A. R. Champneys, T. F. Fairgrieve, Y. A. Kuznetsov, B. Sandstede, and X.-J. Wang, *AUTO97: Continuation and bifurcation software for ordinary differential equations*, Tech. report, Department of Computer Science, Concordia University, Montreal, Canada, 1997, Available at `ftp://ftp.cs.concordia.ca/pub/doedel/auto`.

[10] G. Fibich and D. Levy, *Self-focusing in the complex Ginzburg-Landau limit of the critical nonlinear Schrödinger equation*, Phys. Lett. A **249** (1998), no. 4, 286–294.

[11] G. Fibich and G. Papanicolaou, *Self-focusing in the perturbed and unperturbed nonlinear Schrödinger equation in critical dimension*, SIAM J. Appl. Math. **60** (1999), no. 1, 180–243.

[12] E. Hairer, S.P. Nørsett, and G. Wanner, *Solving Ordinary Differential Equations I. Nonstiff Problems*, second ed., Springer Series in Comput. Mathematics, vol. 8, Springer-Verlag, 1993, Available at `http://www.unige.ch/math/folks/hairer/software.html`.

[13] W. Huang, Y. Ren, and R. Russell, *Moving mesh methods based on moving mesh partial differential equations*, Jnl. of Comp. Phys. **113** (1994), no. 2, 279–290.

[14] N. Kopell and M. Landman, *Spatial structure of the focusing singularity of the nonlinear schrödinger equation: a geometrical analysis*, SIAM J. Appl. Math. **55** (1995), no. 5, 1297–1323.

[15] B.J. LeMesurier, G.C. Papanicolaou, C. Sulem, and P. L. Sulem, *Local-structure of the self-focusing singularity of the nonlinear Schrödinger-equation*, Physica D **32** (1988), no. 2, 210–226.

[16] K. McLeod and J.Serrin, *Uniqueness of positive radial solutions of $\delta u + f(u) = 0$ in r^n*, Arch. Rational Mech. Anal. **99** (1987), no. 2, 115–145.

[17] A. Mielke, *The Ginzburg-Landau equation in its role as a modulation equation*, in Handbook of dynamical systems **2**, North-Holland (2002), 759–834.

[18] A.C. Newell and J.A. Whitehead, *Finite bandwidth, finite amplitude convection*, J. Fluid Mech. **28** (1969), 279–303.

[19] P. Plecháč and V. Šverák, *On self-similar singular solutions of the complex Ginzburg-Landau equation*, Comm. Pure Appl. Math. **54** (2001), 1215–1242.

[20] M.J.D. Powell, *A hybrid method for nonlinear equations*, Numerical Methods for Nonlinear Algebraic Equations (P. Rabinowitz, ed.), Gordon and Breach, 1988.

[21] V. Rottschäfer and T. Kaper, *Blow-up in the nonlinear Schrödinger equation near critical dimension*, J. Math. Anal. Appl. **268** (2002), no. 2, 517–549.

[22] ———, *Geometric theory for multi-bump, self-similar, blow-up solutions of the cubic nonlinear Schrödinger equation*, Nonlinearity **16** (2003), no. 3, 929–961.

[23] K. Stewartson and J. Stuart, *A nonlinear instability theory for a wave system in plane Poiseuille flow*, J. Fluid Mech. **48** (1971) 529–545.

[24] C. Sulem and P. L. Sulem, *The Nonlinear Schrödinger Equation*, Appl. Math. Sci., vol. 139, Springer-Verlag, Berlin, 1999.